original research

Canadian Undergraduate Physics Journal

Journal Canadien des Étudiants en Physique

VOLUME III ISSUE 2 JANUARY 2005

Numerical study of quadrupole magnetic traps for neutral atoms: anti-Helmholtz coils and a U-chip

Hyun Youk

Department of Physics, University of Toronto. Currently at Johns Hopkins University (hyun.youk@jhu.edu)

Received 1 November 2004; Accepted 8 December 2004

Abstract

Anti-Helmholtz coils and micro-fabricated chips are used for magnetically trapping neutral atoms in forming Bose-Einstein condensates and Fermi degenerate gases. Although they are widely used, literature dealing with a detailed numerical study of the magnetic fields involved in these traps is incomplete. Analytical and numerical investigations were carried out to study the physical properties of the magnetic fields produced by the anti-Helmholtz coils and a U-chip. The roles played by electric current and geometric aspects of these magnetic traps are emphasized through numerical modelling.

Introduction

The first experimental realization of a Bose-Einstein Condensate (BEC) occurred in 1995, launching an intense study of ultra-cold atoms which continues to this day[1,2,3,4]. BEC is a system in which a macroscopic number of bosons are put into a common ground state as a result of Bose-Einstein statistics. Producing a BEC in a laboratory allows for the study of fundamental issues in quantum mechanics and opens new doors for future investigations.

Aside from the fundamental physics explored using a BEC, the experimental techniques involved in forming a BEC have drawn considerable interest. One reason is because these techniques are used for other quantum optics experiments. Variations and improvements of the original techniques of Anderson *et al.* have been used to form BECs and related forms of degenerate gases[4,5]. To produce a BEC in an atomic gas, the atoms are typically cooled to a temperature on the order of a μK and are spatially confined to maintain a required number density[6] of about 10^{14} cm^{-3}. This is required so that the average thermal de Broglie waves of the individual particles overlap. This spatial confinement also keeps the particles away from the warm walls of the vacuum chambers in which BECs are formed, which helps them achieve equilibrium faster. A technique known as magnetic trapping is employed to achieve this spatial confinement. In addition to spatial confinement, magnetic traps play an important role in the cooling of particles in processes known as laser cooling and evaporative cooling[7,8,9,10,11].

An atom with magnetic moment μ_B and a z-component spin number of m_z has a potential energy $E(m_z) = gm_z\mu_B B$ where B is the applied magnetic field and g is the Lande g-factor. If gm_z is positive, then the atom is said to be in a weak-field-seeking state. For this state, a magnetic field with a local minimum confines the atom in the potential well. The potential near the local minimum can be approximated as a quadratic well. An atom with a strong-field-seeking state where gm_z is negative cannot be trapped using a static magnetic field because no local maximum of magnetic field can exist according to Maxwell's equations[12].

Magnetic traps can be divided into two categories. Quadrupole traps are those whose local minimum of the interaction potential, $E(m_z)$, is zero. The other type is one with a local minimum of $E(m_z)$ being nonzero (Ioffe-Pritchard-type trap)[8]. It should be noted that a quadrupole trap alone cannot be used to form a quantum degenerate gas due to Majorana spin flips that occur at the zero of the trap. Nevertheless, it serves as a backbone to some of the traps that are used for formation of degenerate gases. In this paper, we present a detailed numerical study of two magnetic traps that fall into the former category: anti-Helmholtz coils and a U-chip. While literature dealing with the properties of these traps exists, published studies dealing purely with the set of field equations describing the traps do not. In addition, the role that the geometric aspect of the trap and the electric current play, via a scaling rule, in determining their properties have not been addressed. New atom trapping experiments must calculate the necessary field equations for the trap being designed. Indeed, the numerical model presented in this paper was developed when the ultra-cold atoms lab led by Joseph Thywissen at the University of Toronto began its atom trapping experiment in May of 2003. This study provides a recipe for magnetic traps, detailing a set of key field expressions that can be quickly referred to when designing a magnetic trap.

Anti-Helmholtz coils

FIELD EQUATIONS

Anti-Helmholtz coils were used in the first generation of BEC experiments. Migdall *et al.* outlines the key features of anti-Helmholtz coils in an experimental setup[13]. In their experiment, two coaxial loops having a radius of 2.7 cm, a separation distance of about 3.7 cm, and a current of 12.58 A were used[13]. Although the features of their particular trap are outlined in their paper, the properties of coils with arbitrary current, radii, and separation distance are not discussed. In the present study, these properties are derived for coils with arbitrary parameters.

Typically, one or more pairs of anti-Helmholtz coils are wrapped around the vacuum cell in which atoms are trapped. The size of the anti-Helmholtz coils varies depending on the experimental setup. We assume the coil is made up of a single wire but in an actual experiment, a coil consists of many wires wound around a cylindrical spool. However, our model is still applicable to such an experimental setting via the superposition principle.

A calculation of the magnetic field $\mathbf{B}_{\text{along } z}(z)$ along the z-axis (the axis of symmetry) of a pair of anti-Helmholtz coils, as shown in Figure 1, yields

$$\mathbf{B}_{\text{along } z}(z) = \frac{\mu_0 I}{2a}\left(\frac{1}{\left(1+\left(\frac{z}{a}-\frac{d}{2a}\right)^2\right)^{3/2}} - \frac{1}{\left(1+\left(\frac{z}{a}+\frac{d}{2a}\right)^2\right)^{3/2}}\right)\hat{\mathbf{z}}, \tag{1}$$

where I is the current flowing through the two coils, a is the radius and d is the separation distance. The current in each coil is flowing in opposite directions with respect to one another. Introducing the following proportionality factors

$$\alpha = \frac{2z}{a}, \quad \beta = \frac{d}{2a}, \quad \lambda = \frac{I}{2a\pi}, \tag{2}$$

Equation (1) can be written as

$$\mathbf{B}_{\text{along } z}(\alpha,\beta) = \mu_0\pi\lambda\left(\frac{1}{\left(1+\left(\frac{\alpha}{2}-\beta\right)^2\right)^{3/2}} - \frac{1}{\left(1+\left(\frac{\alpha}{2}+\beta\right)^2\right)^{3/2}}\right)\hat{\mathbf{z}}. \tag{3}$$

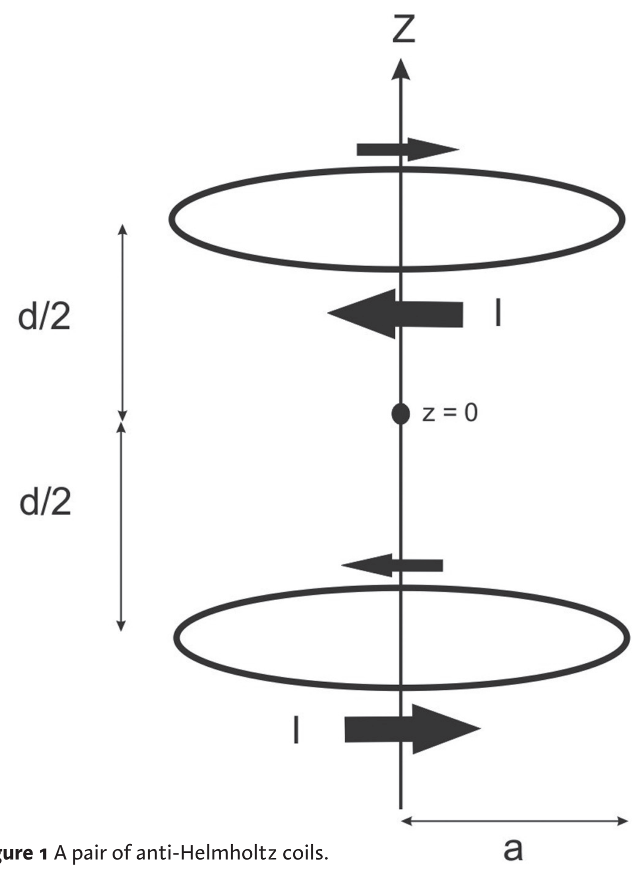

Figure 1 A pair of anti-Helmholtz coils.

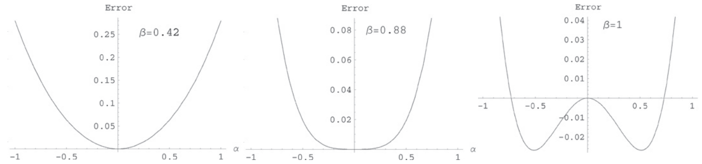

Figure 2 Morphism of the error curve associated with Equation (4) at three values of β: 0.42, 0.88, 1.0.

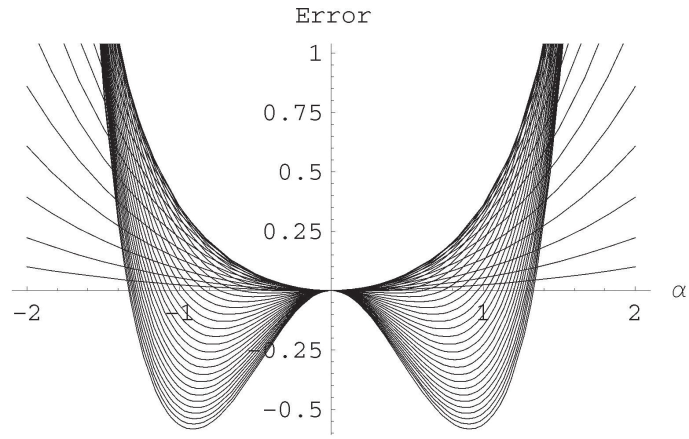

Figure 3 Family of error curves associated with Equation (4). Each curve corresponds to a different value of β.

α and β are geometric properties of the coils, while λ is the uniform circular current density. Since the field is zero at the origin, this is the location of the minimum of $E(m_z)$, and is thus the only place where the atoms can be trapped along the axis of symmetry. By first-order linear approximation for $z \ll a$ and $z \ll d$, the field along the z-axis is

$$\mathbf{B}_{\text{approx}}(\alpha,\beta) = \mu_0\pi\lambda\frac{6\beta^2\alpha}{(1+\beta^2)^{5/2}}\hat{\mathbf{z}}. \tag{4}$$

Numerical analysis indicates that the linear approximation deviates by less than 2% if $\alpha < 0.2$ with β is in the interval [0.4, 1.0]. These values of α

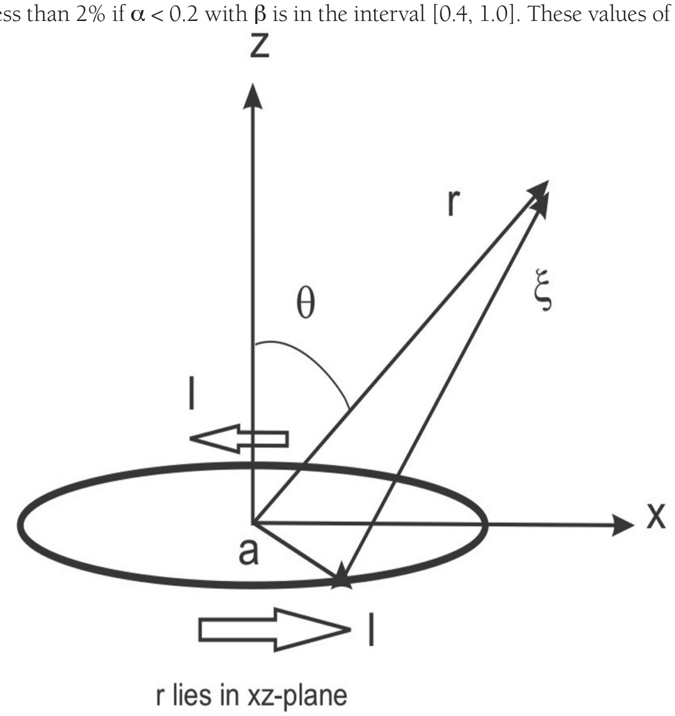

Figure 4 Parametrization for the *xz*-plane shown for a single coil of radius *a*, carrying current *I*.

and β are of interest for atom-trapping. As β increases from 0.4 to approximately 0.74, the error curve transitions into a tighter quadratic shape. As β is increased above 0.74, the trough of the field-well flattens out and transitions into a quartic shape. Figure 2 shows this morphism in more detail, while Figure 3 shows the superposition of the the family of error curves for various values of β.

Newton's method can be used to locate the exact maximum field strength locations for various α and β configurations.

For practical purposes, the linear approximation of Equation (4) can be used to find the gradient of the field along the z-axis. It is found to be

$$\left.\frac{dB}{dz}\right|_{z\approx 0} = \frac{48a^2 d\mu_0 I}{(4a^2+d^2)^{5/2}}. \tag{5}$$

The field strength produced by a single coil (shown in Figure 4) is

$$\mathbf{B}_{xz} = \frac{\mu_0 Ia}{2\pi}\left(\int_0^{\pi}\left[\frac{(r\sin(\theta)\cos(\phi'))}{\xi^3}\right]d\phi', 0, \int_0^{\pi}\left[\frac{(a-r\sin(\theta)\cos(\phi'))}{\xi^3}\right]d\phi'\right), \tag{6}$$

where $\mathbf{B}_{xz}$ is a vector in Cartesian coordinates and $\xi = \mathbf{r}-\mathbf{a}$. The parameters for the two coils as shown in Figure 5 are used for calculation of the field in the entire space. These parameters are

$$r_1(r,\theta) = \sqrt{\frac{d^2}{4} + r^2 + rd\cos(\theta)}, \tag{7}$$

$$r_2(r,\theta) = \sqrt{\frac{d^2}{4} + r^2 - rd\cos(\theta)}, \tag{8}$$

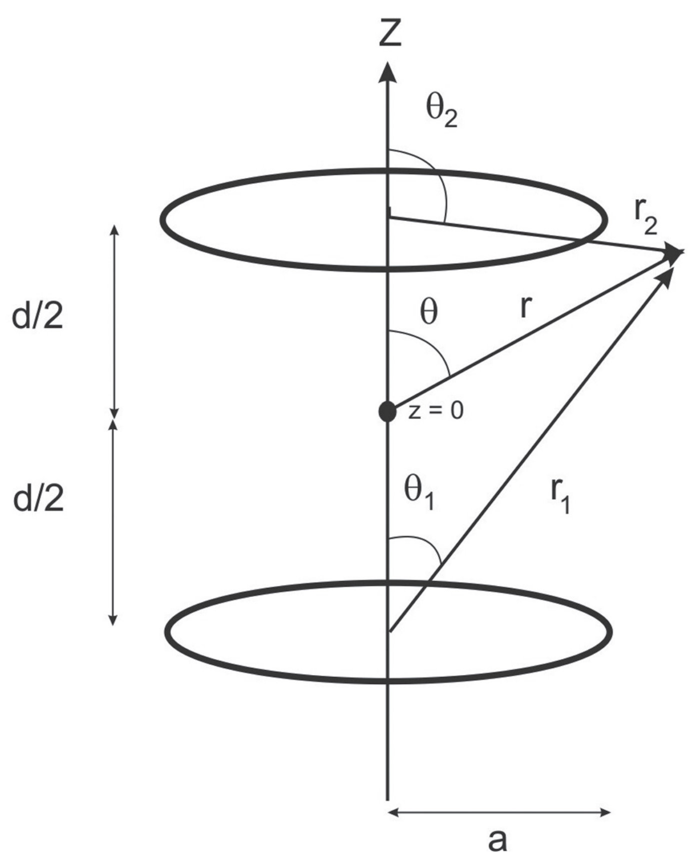

Figure 5 Parametrization for the anti-Helmholtz coils.

$$\theta_1(r,\theta) = \arccos\left(\frac{2r\cos(\theta)+d}{2\sqrt{\frac{d^2}{4}+r^2+rd\cos(\theta)}}\right), \tag{9}$$

$$\theta_2(r,\theta) = \pi - \arccos\left(\frac{d-2r\cos(\theta)}{2\sqrt{\frac{d^2}{4}+r^2-rd\cos(\theta)}}\right). \tag{10}$$

Equation (6), which involves the hypergeometric F_1 function (also called a Gauss or Kummer series), was evaluated numerically to obtain the field strength.

As seen in Figure 6, for a fixed radial distance, the weakest field strength lies in the xy-plane. The contour plot of the magnetic field in the xz-plane is shown in Figure 7. Figure 7 is analogous to Figure 1 in Migdall *et al.*[13], but we have shown the associated field expressions parametrized by α, β and λ. Through numerical expansion, it was found that for $\beta = 0.5$, the field strength in the xy-plane near the trap centre is

$$B_{xy} \approx 0.429\frac{\mu_0 I\rho}{a^2}. \tag{11}$$

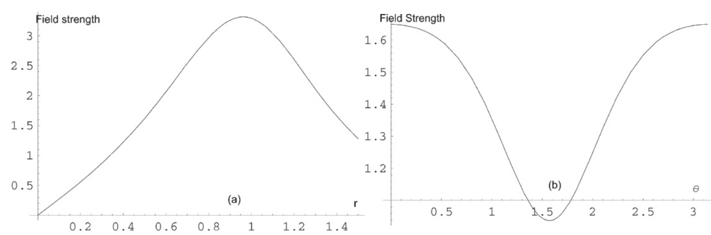

Figure 6 (a) Field strength on a radial line emanating from the origin (on the xy-plane). **(b)** Strength of the field on the prime meridian of a sphere of radius $r = 0.35a$. Note that the field strength is weakest at the equator.

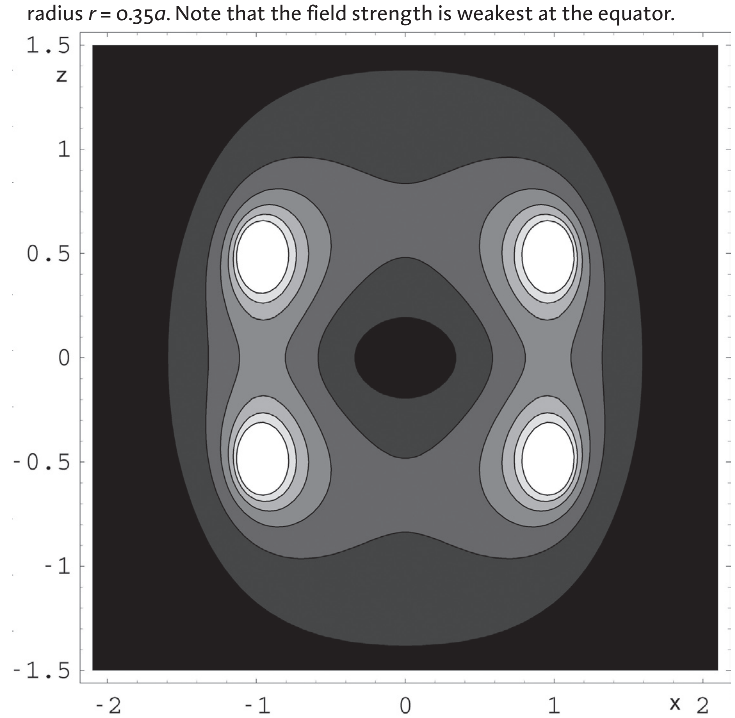

Figure 7 Contour plot indicating the strength of the quadrupole field produced by the anti-Helmholtz coils (with β=1) on the xz-plane. Darker shades indicate regions of weaker field strength. The four white regions are where the coils emerge on the xz-plane, and indicate the region of the strongest field strength.

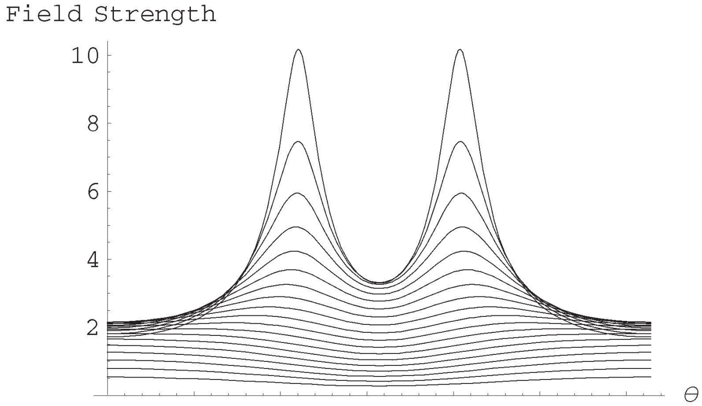

Figure 8 Field strength on spheres of varying radii. Each curve corresponds to a different sphere centered about the origin.

By cylindrical symmetry, the radial gradient of the field in the *xy*-plane at the origin is exactly half that along the *z*-axis. Equation (11) indicates otherwise because it is a linear approximation of the field in the *xy*-plane near the origin. Thus, the discarded higher order terms contribute to numerical errors.

RESULTS AND DISCUSSIONS

Equation (3) shows that the field produced by the coils is not determined by individual parameters such as radius, separation distance, or current, but by the relationship between these parameters as characterized by α, β, and λ. Furthermore, Equation (3) shows that the locations of the maxima of the field are determined only by the coils' geometry, and not by the current.

The trap depth of anti-Helmholtz coils was deduced numerically. According to Figure 8, for the surface of a sphere centered at the origin, the weakest field is on its equator. Thus a trap depth is the field strength at the saddle point of $E(m_z)$ on some sphere of radius r_{saddle}. In this situation, particles with an average thermal energy below the interaction energy, corresponding to the saddle point of the energy curve, will not be able to escape from this sphere.

The saddle point of trapping potential $E(m_z)$ was determined graphically. Literature on anti-Helmholtz coils does not provide the numerical value of the saddle point field intensity[13,14]. The graphical solution yields $r_{saddle} \approx 0.96152$ and $\theta = \pi/2$ radians to be the approximate location of the trap-depth for $\beta = 0.5$. The corresponding magnetic field strength is approximately 3.30031 (units).

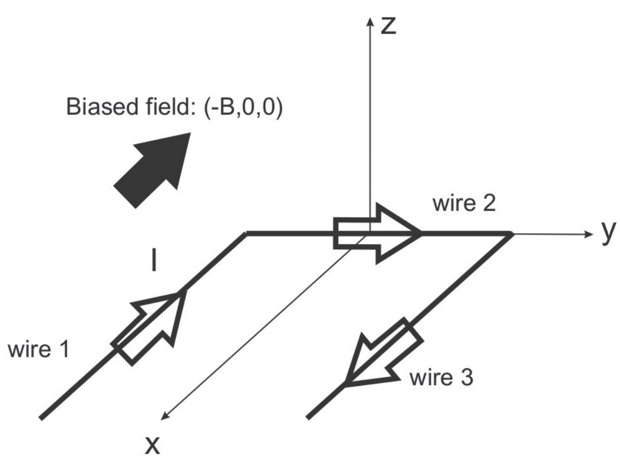

Figure 9 U-chip carrying current *I* lying on the *xy*-plane. Note that the biased field is in the negative *x*-direction. The length of wires 1 and 3 is 2*l* while the length of wire 2 is 2*w*.

The "units" above is undetermined unless a length unit corresponding to the radius *a* is specified. Since the unit for magnetic field is force per unit current per unit length, where force is given in N and current in A, this leaves unit length to be specified. This length unit can be anything one chooses. For instance, we can define 1 unit of length to be π meters. Once the unit length has been specified, all other parameters, such as r_{saddle}, must adhere to the same unit. For simplicity, we set $a = 1$ (length unit). The value of 3.30031 has a unit corresponding to this choice of length. The numerical value 3.30031 does not change regardless of this choice. With $\beta = 0.5$, the field strength at the saddle point is

$$\left|\mathbf{B}_{\text{saddle}}\right| \approx \frac{\mu_0 I(3.30031)(\text{units})}{2\pi}. \tag{12}$$

The corresponding trap-depth energy (in K) is

$$E_{\text{trap-depth}} = \frac{(1.90403\times 10^{-31})m_z\lambda}{k_B}, \tag{13}$$

where k_B is the Boltzman's constant. It is useful to note that in Equation (13), the dynamic parameter *I* is coupled with the geometric parameter *a*, and this ratio λ determines the trap depth, not the individual values of *a* and *I*. This is valuable information when implementing a magnetic trap in an experiment since the heating in a coil is determined by the radius of the coil, but not by the separation distance. Hence, by reducing the radius of the coil while keeping β constant, the same trap strength is produced while reducing the heating of the wires.

U-chip with biased field parallel to its surface

FIELD EQUATIONS

Atoms can be trapped above a surface on which a planar current runs through. One such example is the U-chip, as shown in Figure 9. One of its advantages is that it is more compact than an anti-Helmholtz coil, and can be directly placed inside a vacuum cell where the atoms are trapped.

To study the U-chip, a calculation of the magnetic field produced by a single wire is necessary. The static magnetic field produced by a single wire lying on the *z*-axis between $z = -l$ and $z = l$ carrying a current *I* in the positive *z*-direction is

$$\mathbf{B}(z,r) = \frac{\mu_0 I}{4\pi}\left(\frac{l+z}{z\sqrt{(z+l)^2+r^2}} - \frac{l-z}{r\sqrt{(z-l)^2+r^2}}\right)\hat{\boldsymbol{\phi}}, \tag{14}$$

where *r* is the azimuthal distance from the *z*-axis, and $\hat{\phi}$ is the azimuthal vector in cylindrical coordinates.

The U-chip consists of the field generated by its U-shaped current carrying wire and a biased external magnetic field[12]. As shown in Figure 9, the width of chip is 2*w* and its length is 2*l*. For the model presented in this paper, a biased field is oriented in the negative *x*-direction as shown in Figure 9. Trap centres can only be formed at locations above the chip where the vertical fields produced by the U-wire configuration are zero. Since wire 2 does not produce any *y*-component fields, trap centres only form on the *xz*-plane. Using Equation (14), it is seen that the *z*-components of the fields produced by wires 1 and 3 cancel each other out when α and β satisfy

$$\left(\frac{1}{1+\beta^2}\right)\left|\alpha + \frac{(2\gamma-\alpha)\sqrt{1+\alpha^2+\beta^2}}{\sqrt{1+\beta^2+(2\gamma-\alpha)^2}}\right| = \frac{-\alpha}{\alpha^2+\beta^2}, \tag{15}$$

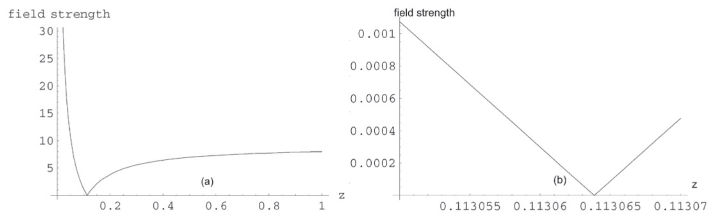

Figure 10 Strength of the field produced by the U-chip. These plots show the field strength along the z-axis about the trap centre. **(a)** With $\alpha = -0.02$, the trap centre is marked by a discontinuity. **(b)** Zooming into the region near the trap centre, we see an approximately linear behaviour of the field strength, characteristic of quadrupole traps.

where the following proportionality factors are used:

$$\alpha = \frac{x}{w}, \qquad \beta = \frac{z}{w}, \qquad \gamma = \frac{l}{w}. \tag{16}$$

α must be negative since the trap centre can only be formed for $x < 0$. A variant of the bisection method was used to determine β.

If γ is increased while α is kept fixed, it is found that β is decreased. To understand why this happens, let B_{13} be the strength of the downward z-component field on the xz-plane due to wires 1 and 3. Let B_2 be the strength of upward z-component field on the same plane due to wire 2. Increasing γ corresponds to either decreasing the width w or increasing the length l. In either case, the lengths of wires 1 and 3 relative to wire 2 is increased. In turn, current in wires 1 and 3 have a longer path to traverse than in wire 2, and hence B_{13} is strengthened. Thus, the gap between the strengths of two fields is decreased. Therefore, it takes less height above the chip for B_2 and B_{13} to "catch up" with each other. Hence trap centres can be formed closer to the chip surface as γ is increased.

For some values of α, corresponding values of β satisfying Equation (15) do not exist. In particular, given a U-chip with fixed l and w, there always exists a critical height z_c, above which a trap centre cannot be formed, and below which a trap centre can always be formed. The main reason behind this is that the rate at which vertical field strength decreases along the negative x-direction is different from the rate at which it decreases along the z-direction. Below z_c, there exists a curve joining the origin (0,0) to a point at z_c, along which B_{13} and B_2 decrease at the same rate. This is the curve on which trap centres lie. Such a curve does not exist above z_c. This is the reason for the existence of maximum trap centre height.

RESULTS AND DISCUSSIONS

Similar to the anti-Helmholtz coils, an important scaling rule for U-chips was deduced through numerical modelling. The relative locations at which the z-component of the field is zero is invariant under changes in current. Since the field strength is proportional to the current, the z-component of the magnetic field would change by the same factor as I if the current is changed. Hence, the trap centres remain at the same position above the chip if both the current and the biased field strength are changed by the same factor. The zero magnetic field locations in the z-direction are a geometric property of the chip, and do not depend on the current and the biased field strength. Thus, specifying the length and width of the U-chip also specifies the places above the chip where the zeroes of the trap are formed.

The plots in Figure 10 indicate that close to the trap centre, the field strength of the U-chip changes approximately linearly.

Reichel[14] states that the gradient of the field along the z-axis is approximately

$$\frac{dB}{dz} \propto B_{\text{biased}}^2. \tag{17}$$

α	z (cm)	B_{biased} (G)	dB/dz (G/cm)
−0.001	0.02508	39.8033	1588.26
−0.01	0.07962	12.3788	157.133
−0.02	0.11306	8.59279	77.5617
−0.07	0.2161	4.18832	20.5284
−0.08	0.23213	3.84633	17.6556
−0.1	0.26197	3.31595	13.6258
−0.3	0.50597	4.18832	2.98425

Table 1 Gradient of field strength along the z-axis ($\gamma = 1$, $I = 5\,\text{A}$, $2w = 1.5\,\text{cm}$)

This approximation assumes that along the z-axis emanating from the fixed $x = \alpha w$ location, the z-component field strength is weaker than the x-component field, since the approximations given by Reichel are exact only for a single straight wire with a biased field perpendicular to it. Reichel's approximation and the results from the present numerical study are shown in Table 1.

Typically, the dimensions of the chip are on the order of millimetres but the length scale in Table 1 is in centimetres. However, as explained in the case of anti-Helmholtz coils, changing the length scale corresponds to changes in the units given in Table 1, which can be determined by dimensional analysis. $\gamma = 1$ was chosen for simplicity.

Given a U-chip with fixed dimensions and a range of currents, there is a fixed range of biased field strengths that can be used to create trap centres above the chip. For a biased field strength outside of this range, no trap centre can be created above the chip with any given l and w.

Conclusions

These numerical models describe scaling rules governing a U-chip and anti-Helmholtz coils not detailed in the already extensive literature on magnetic traps. Since most literature on magnetic traps focuses almost exclusively on the experimental setup and usage of the trap rather than the detailed properties of the fields produced by them, numerical modelling of these traps has to be carried out from scratch at the beginning of every atom trapping experiment. By presenting a set of numerical field equations, such steps can be minimized or avoided altogether. In addition, the scaling rules for these traps have shown the roles that electric current and geometric aspects of the traps play, both independently and in conjunction with each other, in determining the properties of the trapping field.

Acknowledgements

The author thanks Joseph Thywissen for guidance and providing the facility on which the numerical studies were done. This work would not have been possible without the generous funding from NSERC in the form of an Undergraduate Summer Research Award, and the author gratefully acknowledges its financial support.

References

[1]M.H. Anderson, *et al.* "Observation of Bose-Einstein condensation in a dilute atomic vapor." *Science.* (1995) **269**, pp. 198–201.

[2]K.B. Davis, *et al.* "Bose-Einstein condensation in a gas of sodium atoms." *Physical Review Letters.* (1995) **75** (4), pp. 3969–3973.

[3]C.C. Bradley, *et al.* "Evidence of Bose-Einstein condensation in an atomic gas with attractive interactions." *Physical Review Letters.* (1995) **75** (9), pp. 1687–1690.

[4]C.A. Sackett, *et al.* "Bose-Einstein condensate of lithium." *Applied Physics B.* (1997) **65**, pp. 433–440.

[5] B. DeMarco and D. Jin. “Exploring a quantum degenerate gas of fermionic atoms.” *Physical Review A*. (1998) **58** (4), pp. R4267–R4270.

[6] W. Ketterle, D.S. Durfee and D.M. Stamper-Kurn. “Making, probing, and understanding Bose-Einstein condensates.” *Proceedings of the 1998 Enrico Fermi summer school on Bose-Einstein condensation*. Varenna, Italy. (1999).

[7] W.D. Phillips, J.V. Prodan and H.J. Metcalf. “Laser cooling and electromagnetic trapping of neutral atoms.” *Journal of the Optical Society of America B*. (1985) **2** (11), p. 1751.

[8] T. Bergeman, G. Erez and H. Metcalf. “Magnetostatic trapping fields for neutral atoms.” *Physical Review A*. (1987) **35** (4), pp. 1535–1546.

[9] A. Griffin, D.W. Snoke and S. Stringari. *Bose-Einstein Condensation*. Cambridge University Press: Cambridge. (1996) p. 131.

[10] J.T.M. Walraven. “Atomic hydrogen in magnetostatic traps.” *Quantum Dynamics of Simple Systems*, G.L. Oppo, S.M. Barnett, E. Riis and M. Wilkinson, Eds. Institute of Physics Publication: Bristol. (1996) p. 315.

[11] W. Ketterle and N.J. van Druten. “Evaporative cooling of atoms.” *Advances in Atomic, Molecular, and Optical Physics*. Academic Press: San Diego. (1996) **37**, p. 181.

[12] W. H. Wing. “On neutral particle trapping in quasistatic electromagnetic fields.” *Progress in Quantum Electronics*. (1984) **8** (3), pp. 181–199.

[13] A.L. Migdall, *et al*. “First observation of magnetically trapped neutral atoms.” *Physical Review Letters*. (1985) **54** (24), pp. 2596–2599.

[14] J. Reichel. “Microchip traps and Bose Einstein condensation.” *Applied Physics B*. (2002) **75** (4), pp. 469–487.